9-1-2010

Optimal Guidance of a Relay Aircraft to Extend Small Unmanned Aircraft Range

Meir Pachter
Air Force Institute of Technology

John Hansen

David R. Jacques
Air Force Institute of Technology

Paul Blue

Recommended Citation

Pachter, M., Hansen, J., Jacques, D., & Blue, P. (2010). Optimal Guidance of a Relay Aircraft to Extend Small Unmanned Aircraft Range. International Journal of Micro Air Vehicles, 2(3), 157–180. https://doi.org/10.1260/1756-8293.2.3.157

Optimal Guidance of a Relay Aircraft to Extend Small Unmanned Aircraft Range[1]

Meir Pachter[2], John Hansen[3], David Jacques[4] and Paul Blue[5]
Air Force Institute of Technology, Wright-Patterson AFB, OH, 45433

ABSTRACT

This paper developed guidance laws to optimally and autonomously position a relay Micro Aerial Vehicle (MAV) to provide an operator with real-time Intelligence, Surveillance, and Reconnaissance (ISR) by relaying communication and video signals from a rover MAV to the base, thus extending the rover's reach. The ISR system is comprised of two MAVs, the Relay and the Rover, and a Base. The Relay strives to position itself so as to minimize the radio frequency (RF) power required for maintaining communications between the Rover and the Base, while the Rover performs the ISR mission, which may maximize the required RF power. The optimal control of the Relay MAV then entails the solution of a differential game. Applying Pontryagin's Maximum Principle yields a standard, albeit nonlinear, Two-Point Boundary Value Problem (TPBVP). Suboptimal solutions are first obtained as an aid in solving the TPBVP which yields the solution of the differential game. One suboptimal approach is based upon the geometry of the ISR system: The midpoint between the Rover and the Base is the ideal location which minimizes the RF power required, so the Relay heads toward that point—assuming that the Rover is stationary. At the same time, to maximize the rate of required RF power, the Rover moves in the opposite direction of the Relay—assuming the Relay is stationary. These are optimal strategies in the end-game, but it is suboptimal to use them throughout the game. Another suboptimal approach investigated envisions the Rover to remain stationary and solves for the optimal path for the Relay to minimize the RF power requirement. This one-sided optimization problem is analyzed using a Matlab-based optimization program, GPOCS, which uses the Gauss pseudospectral method of discretization. The results from GPOCS corroborated with the geometry-based suboptimal Relay strategy of heading straight toward the midpoint between the Rover and the Base. The suboptimal solutions are readily implementable for real-time operation and are used to facilitate the solutions of the TPBVP.

NOMENCLATURE

B	=	Base
E	=	RElay MAV
H	=	Hamiltonian
M	=	Midpoint Between Rover and Base
O	=	ROver MAV
T	=	Planning Horizon
x	=	State Vector
y	=	Cost

---

[1] The views expressed in this paper are those of the authors and do not reflect the official policy or position of the United States Air Force, Department of Defense, or the United States Government.

A previous version of this work was presented at the AIAA GNC conference in August 2008.

[2] Professor, meir.pachter@afit.edu

[3] 2nd Lt., U.S. Air Force, john.hansen.5@us.af.mil

[4] Associate Professor, david.jacques@afit.edu

[5] LtCol, U.S. Air Force, paul.blue@us.af.mil

E_c = Relay Location Closest to Base Along Optimal Guidance Path
r_E = Distance of Relay MAV from Base
r_O = Distance of Rover MAV from Base
t = Time
t_c = Conjugate Time
T_c = Maximum Planning Horizon
V_E = Velocity of Relay
V_O = Velocity of Rover
X_0 = Initial Value of Parameter X
X_k = Value of Parameter X at Iteration Step k
α = Speed Ratio $(\alpha = V_O/V_E)$
θ = Included Angle of the Radials From the Base to the Relay and the Rover
λ = Co-State Vector
φ = Relative Course Angle of Rover
ψ = Relative Course Angle of Relay

1. INTRODUCTION

Unmanned Aerial Vehicles (UAVs) are becoming more prevalent in military operations. UAVs vary in size and mission. Some UAVs are the same size as aircraft, whereas others are man-portable and can be carried in a backpack. These man-portable Micro-UAVs (MAVs) utilized by small tactical units are not supported by satellite communications and typically use line-of-sight radio frequency (RF) modems. Their RF power is somewhat limited by the battery output/payload of the aircraft. The MAVs considered in this paper are utilized for Intelligence, Surveillance and Reconnaissance (ISR) and will therefore be referred to as ISR MAVs or as Rovers.

In order to maintain communications/connectivity/controllability with deployed ISR MAVs/Rovers a relay is used to extend the line-of-sight distance between the Rover and the Base station. This paper focuses on developing guidance laws to optimally position an autonomous Relay MAV to provide the operator at the Base with real-time ISR by relaying communication and sensor data between the operator at the Base and the Rover.

The cooperative control of networked MAVs is an area of significant interest [5, 6, 7, 8, 9]. Recent studies have applied various mobility control laws as a means of optimizing network communications for reliability and robustness. For example, in [1], Dixon and Frew use an extremum seeking controller for mobile communication nodes in order to maximize the signal-to-noise ratio of a network; in [2], Goldenberg et al. have shown that communication nodes should be evenly spaced on the line between the source and destination in order to minimize the energy cost of communicating between the two. This paper offers an alternative approach for optimally positioning the communication node (the Relay) based on posing a differential game: The autonomous Relay strives to position itself such that the RF power required for maintaining communications is minimized, whereas the (worst case) Rover strives to position itself such that the RF power is maximized. The optimal control of the Relay MAV then entails the solution of a differential game. Applying Pontryagin's Maximum Principle yields a standard, albeit nonlinear, Two-Point Boundary Value Problem (TPBVP). Suboptimal Relay and Rover strategies are provided. These will serve as a first guess in solving the TPBVP which yields the optimal strategies.

The results herein will be presented in non-dimensional form so as to make them applicable for a wide variety of UAV applications. An assumption is made, and stated here, that the resulting paths are flyable by the candidate vehicles. A relaxation of this assumption is possible, but the results here provide limits of performance.

2. ANALYSIS

A planar scenario is considered for this investigation. It is assumed that the rElay (E) MAV is cognizant of the rOver's (O) instantaneous position relative to the Base (B) as well as its own position. It is important to note that the rover is free to move independent of the relay; the relay must compensate for the motion of the rover in a way that minimizes the total RF power required to maintain communication between the base and the rover through the relay system. As far as the RF power requirements are concerned, this is determined by their distance from the Base and the Rover-Relay separation. Thus, the state is the distance r_E of the Relay from the Base, the distance r_O of the Rover to the Base, and the angle θ included between the radials from the Base to the Relay and the Rover. This angle is measured clockwise—see Figure 1. The MAVs have simple motion. The control for each MAV is its relative heading angle measured clock-wise from its radial from the Base. Figure 1 provides a visualization of the kinematics. The equations of motion/dynamics are

$$\left.\begin{array}{ll} \dot{r}_E = V_E \cos\varphi & , \; r_E(0) = r_{E_0}, \; 0 \le \varphi \le \pi \\ \dot{r}_O = V_O \cos\psi & , \; r_O(0) = r_{O_0}, \; 0 \le \psi \le \pi \\ \dot{\theta} = \frac{1}{r_O} V_O \sin\psi - \frac{1}{r_E} V_E \sin\varphi & , \; \theta(0) = \theta_0, \; 0 \le t \le T \end{array}\right\} \tag{1}$$

T is the planning horizon utilized by the optimization algorithm. The cost functional is indicative of the RF power required and is the time averaged sum of the squares of the distance between the Relay and the Rover and between the Relay and the Base:

$$\mathcal{Y} = \int_0^T \left(\overline{EO}^2(t) + \overline{BE}^2(t) \right) dt$$

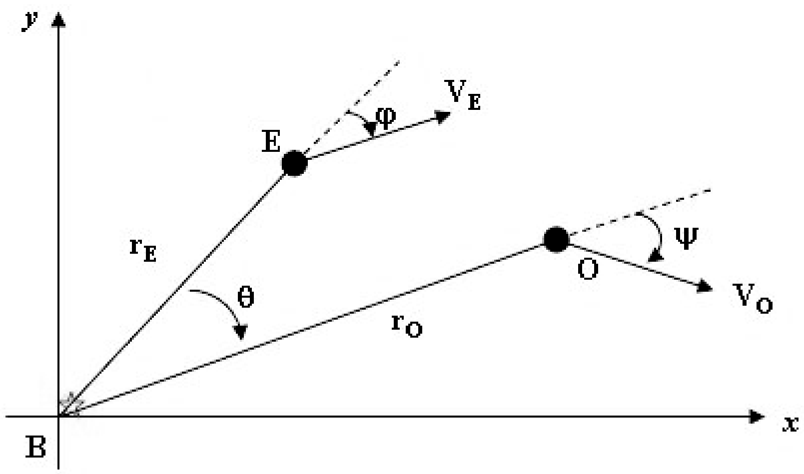

Figure 1. Schematic of Relay System

The points E, B and O in $\mathbf{R}^2$ represent the positions of the Relay, Base and Rover, respectively. These three points form a triangle which can be utilized to calculate the distance $\overline{EO}$ by the law of cosines.

$$\overline{EO}^2(t) = r_E^2 + r_O^2 - 2r_E r_O \cos\theta$$

Hence the cost functional is

$$\mathcal{Y} = \int_0^T \left(2r_E^2 + r_O^2 - 2r_E r_O \cos\theta \right) dt \tag{2}$$

The relay's objective is to minimize the average RF power required for maintaining communications. The control available to accomplish this task is limited to setting the course angle φ of the Relay, while the Rover does whatever it wants, namely, it performs the ISR mission; in a worst case scenario, one might assume that the Rover is working to maximize the cost functional. The optimization problem is then a differential game where the Relay's control is its relative heading φ and the Rover's control is its relative heading ψ.

The optimization problem at hand is analyzed by first non-dimensionalizing the states and the parameters. The velocities are scaled by the velocity of the Relay (V_E), yielding a non-dimensional speed ratio α ($\alpha = \frac{V_O}{V_E}$). The distances are scaled by the product of the velocity of the Relay and the planning horizon ($V_E T$) and time is scaled by the planning horizon (T). Using these non-dimensional variables, the differential game in $\mathbf{R}^2 \times \mathbf{S}^1$ now becomes

$$
\begin{aligned}
&\min_{\varphi}\max_{\psi} \mathcal{Y} = \int_0^T \left(2r_E^2 + r_O^2 - 2r_E r_O \cos\theta\right) dt \\
&\quad s.t. \\
&\quad \dot{r}_E = \cos\varphi \qquad\qquad\qquad , \; r_E(0) = r_{E_0} \\
&\quad \dot{r}_O = \alpha\cos\psi \qquad\qquad\quad\; , \; r_O(0) = r_{O_0} \\
&\quad \dot{\theta} = \tfrac{1}{r_O}\alpha\sin\psi - \tfrac{1}{r_E}\sin\varphi \; , \; \theta(0) = \theta_0 , \; 0 \le t \le 1
\end{aligned}
\tag{3}
$$

where the problem parameter is the speed ratio $\alpha \ge 0$. To solve the differential game, the Hamiltonian is introduced in Eq. (4)

$$
\mathcal{H} = -2r_E^2 - r_O^2 + 2r_E r_O \cos\theta + \lambda_{r_E}\cos\varphi + \lambda_{r_O}\alpha\cos\psi + \lambda_\theta\left(\tfrac{1}{r_O}\alpha\sin\psi - \tfrac{1}{r_E}\sin\varphi\right) \tag{4}
$$

where λ_{r_E}, λ_{r_O} and λ_θ are the co-states.

According to the Pontryagin Maximum Principle [3], the differential equations for the co-states are

$$
\begin{aligned}
\dot{\lambda}_{r_E} &= 4r_E - 2r_O\cos\theta - \frac{\lambda_\theta \sin\varphi}{r_E^2} \;, \; \lambda_{r_E}(1) = 0 \\
\dot{\lambda}_{r_O} &= 2r_O - 2r_E\cos\theta + \frac{\lambda_\theta \alpha\sin\psi}{r_O^2} , \; \lambda_{r_O}(1) = 0 \\
\dot{\lambda}_\theta &= 2r_E r_O \sin\theta \qquad\qquad\qquad , \; \lambda_\theta(1) = 0
\end{aligned}
\tag{5}
$$

and the optimality condition is given by, namely

$$
\begin{aligned}
&\frac{\partial\mathcal{H}}{\partial\varphi} = -\lambda_{r_E}\sin\varphi - \frac{\lambda_\theta\cos\varphi}{r_E} = 0 \\
&\Rightarrow \quad \tan\varphi^* = -\frac{\lambda_\theta}{\lambda_{r_E} r_E}
\end{aligned}
\tag{6}
$$

$$
\begin{aligned}
&\frac{\partial\mathcal{H}}{\partial\psi} = -\lambda_{r_O}\alpha\sin\psi + \frac{\lambda_\theta\alpha\cos\psi}{r_O} : \\
&\Rightarrow \quad \tan\psi^* = \frac{\lambda_\theta}{\lambda_{r_O} r_O}
\end{aligned}
\tag{7}
$$

The second-order sufficiency condition for φ is

$$
\frac{\partial^2\mathcal{H}}{\partial\varphi^2} = -\lambda_{r_E}\cos\varphi + \frac{\lambda_\theta\sin\varphi}{r_E} < 0
$$

and inserting the expression for φ^* from Eq. (6) yields

$$\lambda_\theta + \frac{\left(r_E \lambda_{r_E}\right)^2}{\lambda_\theta} < 0$$
$$\Rightarrow \lambda_\theta(t) < 0 \ \forall \ 0 \le t < 1 \tag{8}$$

Similarly,

$$\frac{\partial^2 \mathcal{H}}{\partial \psi^2} = -\lambda_{r_O} \alpha \cos\psi - \frac{\lambda_\theta \alpha \sin\psi}{r_O} > 0$$

and inserting the expression for ψ^* from Eq. (7) yields

$$\lambda_\theta + \frac{\left(r_O \lambda_{r_O}\right)^2}{\lambda_\theta} < 0$$
$$\Rightarrow \lambda_\theta(t) < 0 \ \forall \ 0 \le t < 1 \tag{9}$$

Furthermore, we also conclude that

$$0 \le \psi^* < \tfrac{\pi}{2} \ \mathit{iff} \ \lambda_{r_O}\left(t\right) < 0$$

The expressions for φ^* and ψ^* given in Eqs. (6) and (7) can also be used to rewrite the state and co-state equations only in terms of the states and co-states. A standard Two-Point Boundary Value Problem (TPBVP) on the interval $t = [0, 1]$ is obtained:

$$\begin{aligned}
\dot{r}_E &= \frac{\lambda_{r_E} r_E}{\sqrt{\lambda_{r_E}^2 r_E^2 + \lambda_\theta^2}} &&, \ r_E(0) = r_{E_0} \\
\dot{r}_O &= \frac{-\alpha \lambda_{r_O} r_O}{\sqrt{\lambda_{r_O}^2 r_O^2 + \lambda_\theta^2}} &&, \ r_O(0) = r_{O_0} \\
\dot{\theta} &= \frac{\lambda_\theta}{r_E \sqrt{\lambda_{r_E}^2 r_E^2 + \lambda_\theta^2}} - \frac{\alpha \lambda_\theta}{r_O \sqrt{\lambda_{r_O}^2 r_O^2 + \lambda_\theta^2}} &&, \ \theta(0) = \theta_0 \\
\dot{\lambda}_{r_E} &= 4 r_E - 2 r_O \cos\theta + \frac{\lambda_\theta^2}{r_E^2 \sqrt{\lambda_{r_E}^2 r_E^2 + \lambda_\theta^2}} &&, \ \lambda_{r_E}(1) = 0 \\
\dot{\lambda}_{r_O} &= 2 r_O - 2 r_E \cos\theta - \frac{\alpha \lambda_\theta^2}{r_O^2 \sqrt{\lambda_{r_O}^2 r_O^2 + \lambda_\theta^2}} &&, \ \lambda_{r_O}(1) = 0 \\
\dot{\lambda}_\theta &= 2 r_E r_O \sin\theta &&, \ \lambda_\theta(1) = 0, \ 0 \le t \le 1
\end{aligned} \tag{10}$$

3. SUBOPTIMAL SOLUTION

Suboptimal solutions are useful in their own right and provide insight into the differential game. Suboptimal solutions can also be used to provide the first guess for solving the TPBVP in Eqs. (10) in order to obtain the optimal strategies for the Relay and Rover.

3.1. Geometric Approach

Using a geometric approach provides a suboptimal but easily implementable solution of the differential game. This approach is suboptimal because the Relay and the Rover each momentarily assume that the other player is stationary when determining their optimal control.

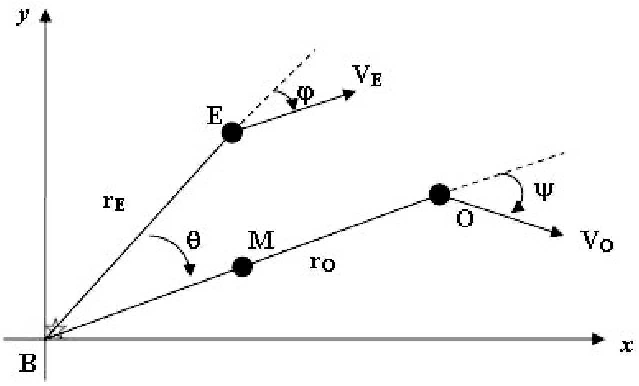

Figure 2. Schematic of Relay System Showing the Midpoint

The geometry of the engagement forms a triangle with vertices E, B and O representing the respective locations of the Relay, Base and Rover (see Figure 2). Let M be the midpoint between the Rover and the Base. Simply rotating the schematic in Figure 2 provides an equivalent schematic (see Figure 3) which is similar to the one analyzed in Appendix A.

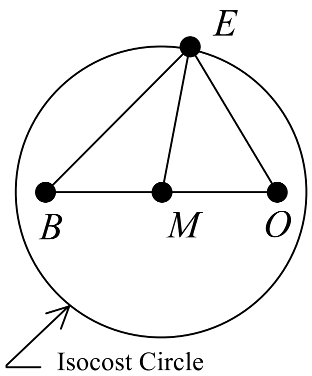

Figure 3. Schematic of Relay System Showing Isocost Circle

If the Rover O were stationary, the loci of constant instantaneous costs for the Relay

$$\mathcal{Y} = \overline{EO}^2 + \overline{BE}^2 = \text{const.}$$

are concentric circles centered at the midpoint M of the segment $\overline{BO}$ and the midpoint M is the Relay location which minimizes the cost[4]. The Relay is on the circumference of said circles, and the instantaneous cost $\mathcal{Y}$ is determined by the position of the Relay. This means that the gradient vector for minimizing cost is in the radial direction. Therefore, the optimal strategy of the Relay is to head toward the midpoint M of $\overline{BO}$.

The optimal control of the Relay is determined using the triangle *ΔBEM*. The distance between *E* and *M* is determined using the law of cosines (just as in determining the distance between *E* and *O* before). The control angle φ is then found and the Relay's strategy is:

$$\varphi^* = \cos^{-1}\left(\frac{r_O\cos\theta - 2r_E}{\sqrt{4r_E^2 + r_O^2 - 4r_E r_O\cos\theta}}\right) \tag{11}$$

As far as the Rover is concerned: the worst case is when the Rover is striving to maximize the cost $\mathcal{Y}$ at each time instant, assuming that the Relay is stationary. This is accomplished by maximizing the rate of the cost $\mathcal{Y}$—the first time-derivative of its integrand. This strategy is equivalent to the optimal solution in the end-game. At time *T-dt* and at state *x*(*T-dt*), all that is left for the Relay and Rover to do is to respectively minimize and maximize the rate of the integrand at that time. The Rover will be using this strategy throughout the game. This proves to be myopic because the Rover is acting as if the game were about to terminate at each time step. Though this may be the optimal strategy in the end-game, it is sub-optimal to employ it for the entire time.

In the case of the system analyzed here, the integrand *L* and the state equations *f* are defined as:

$$L(r_E, r_O, \theta) = 2r_E^2 + r_O^2 - 2r_E r_O\cos\theta$$

$$f(r_E, r_O, \theta) = \begin{pmatrix} \cos\varphi \\ \alpha\cos\psi \\ \frac{1}{r_O}\alpha\sin\psi - \frac{1}{r_E}\sin\varphi \end{pmatrix}$$

The myopic strategy is then given by:

$$\underset{\varphi}{min}\ \underset{\psi}{max}\left[\frac{d}{dt}L(x(t))|_{t=T-dt}\right] = \underset{\varphi}{min}\ \underset{\psi}{max}\left[\frac{\partial L}{\partial x}\ f\right] \tag{12}$$

where

$$\frac{\partial L}{\partial x}\ f = 2\cos\varphi\,(2r_E - r_O\cos\theta) + 2\alpha\cos\psi\,(r_O - r_E\cos\theta) + 2r_E r_O\sin\theta\left(\frac{1}{r_O}\alpha\sin\psi - \frac{1}{r_E}\sin\varphi\right)$$

$$= 2[\cos\varphi\,(2r_E - r_O\cos\theta) - r_O\sin\varphi\sin\theta] + 2\alpha[\cos\psi\,(r_O - r_E\cos\theta) + r_E\sin\theta\sin\psi]$$

Therefore, the Rover's strategy is

$$\frac{\partial}{\partial\psi}\left[\frac{\partial L}{\partial x}\ f\right] = 2\alpha[-\sin\psi\,(r_O - r_E\cos\theta) + r_E\sin\theta\cos\psi]$$

$$\Rightarrow \tan\psi^* = \frac{r_E\sin\theta}{r_O - r_E\cos\theta}$$

which can be applied using an inverse cosine function:

$$\psi^* = \cos^{-1}\left(\frac{r_O - r_E\cos\theta}{\sqrt{r_E^2 + r_O^2 - 2r_E r_O\cos\theta}}\right) \tag{13}$$

This strategy results in the Rover moving directly away from the Relay. Therefore, the suboptimal strategies can be summarized as: the Relay moves directly toward the midpoint M, while the Rover runs away from the Relay. The myopic strategy for the Relay is similarly derived to be

$$\frac{\partial}{\partial \varphi}\left[\frac{\partial L}{\partial x}\ f\right] = 2\ sin\varphi(r_O\ cos\theta - 2r_E) - 2r_O\ sin\theta\ cos\varphi = 0$$

$$\Rightarrow tan\varphi^* = \frac{r_O\ \cos\theta - 2r_E}{r_O \sin\theta}$$

This can also be written using an inverse cosine function:

$$\varphi^* \cos^{-1}\left(\frac{r_O\ \cos\theta - 2r_E}{\sqrt{4{r_E}^2 + {r_O}^2 - 4r_E r_O \cos\theta}}\right)$$

Note that this is the same control law that was found using geometric analysis and the law of cosines (Eq. (11)).

The following numerical results illustrate the evolution of the differential game in the case where the parameter $\alpha = 1$ and the initial conditions are $r_{E_0} = 2$, $r_{O_0} = 4$ and $\theta_0 = \frac{\pi}{6}$; in the game plane, the Rover always starts on the x-axis ($y = 0$). The trajectories show a visualization of the state history, where the Base location is designated by a star at the origin and the final location of each MAV is signified by a triangle. The final midpoint location is designated by a square.

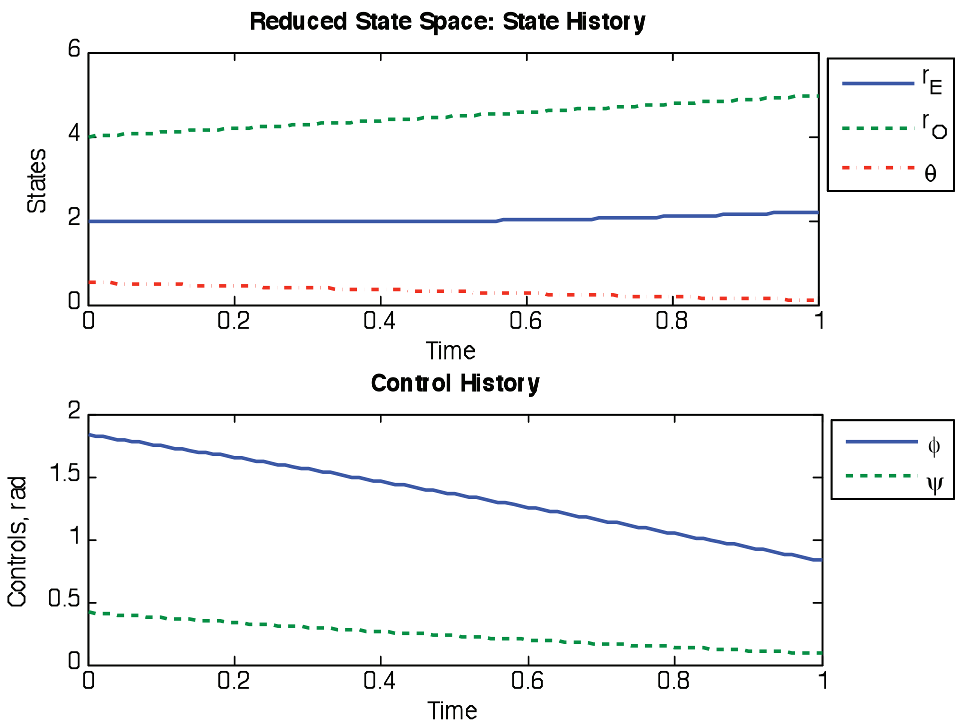

Figure 4. Time History for $\alpha = 1$, $r_{E_0} = 2$, $r_{O_0} = 4$ and $\theta_0 = \frac{\pi}{6}$

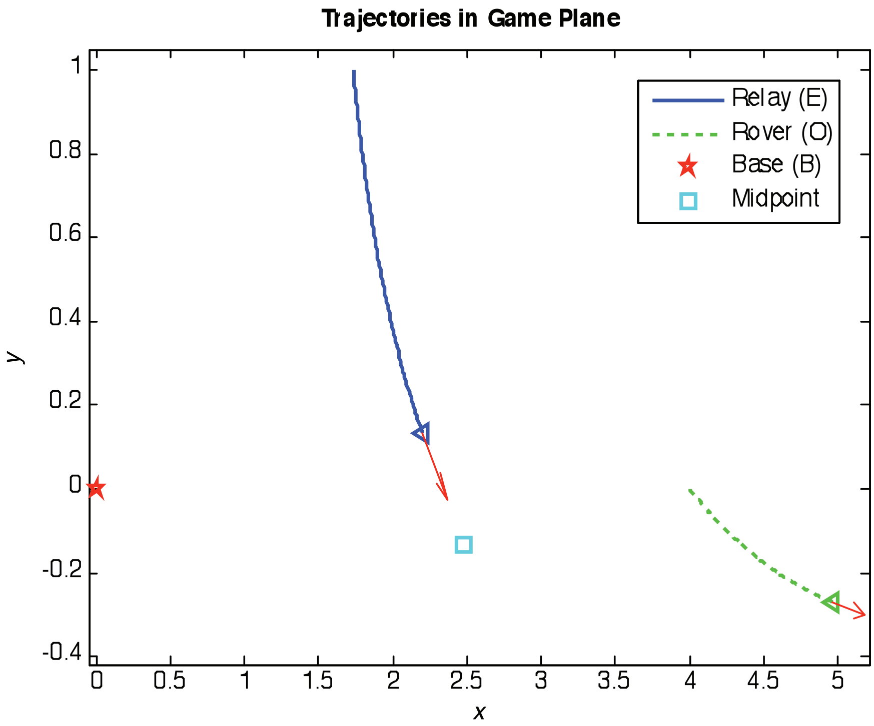

Figure 5. Results for $\alpha = 1$, $r_{E_0} = 2$, $r_{O_0} = 4$ and $\theta_0 = \frac{\pi}{6}$

The following numerical results illustrate the evolution of the differential game in the case where the parameter $\alpha = 1$ and the initial conditions are $r_{E_0} = 1$, $r_{O_0} = 2$ and $\theta_0 = \frac{\pi}{3}$.

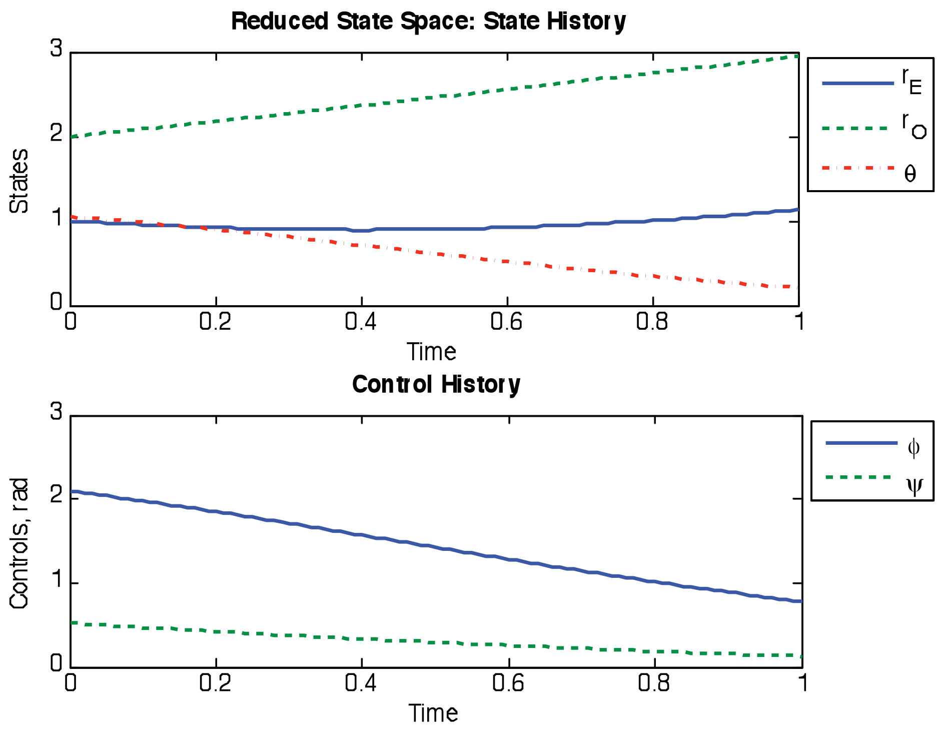

Figure 6. Time History for $\alpha = 1$, $r_{E_0} = 1$, $r_{O_0} = 2$ and $\theta_0 = \frac{\pi}{3}$

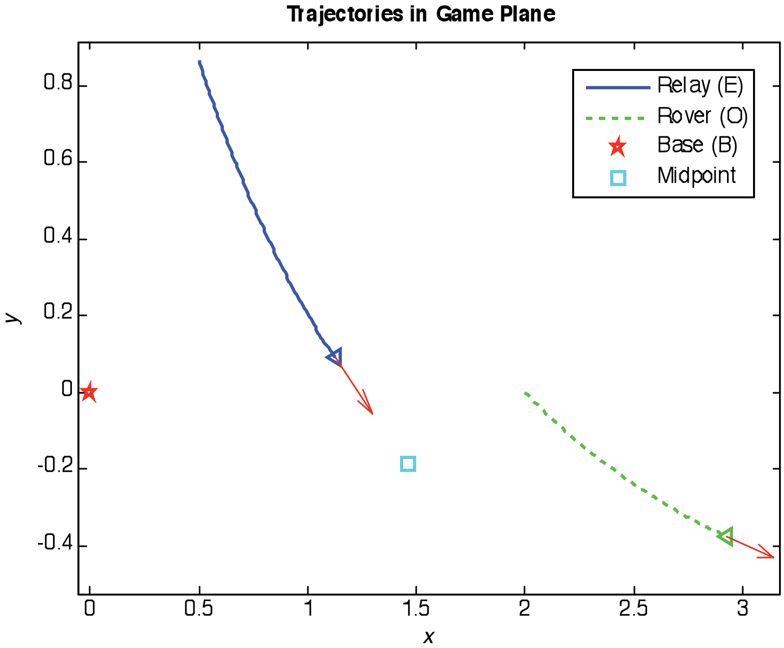

Figure 7. Time History for $\alpha = 1$, $r_{E_0} = 1$, $r_{O_0} = 2$ and $\theta_0 = \frac{\pi}{3}$

The results from the scenarios above show that the system performed exactly as designed.

If T is sufficiently large, the three points E, B and O might become collinear. Once the three points are collinear ($\theta = 0$) the motion is confined to a straight line. The Relay moves toward the midpoint M and the Rover moves away from the Relay. If the speed ratio $\alpha < 2$, the Relay will need to slow down (or chatter) once it reaches the midpoint.

The following numerical results illustrate the evolution of the differential game in the case where the parameter $\alpha = 2$ and the initial conditions are $r_{E_0} = 1$, $r_{O_0} = 2$ and $\theta_0 = \frac{\pi}{6}$.

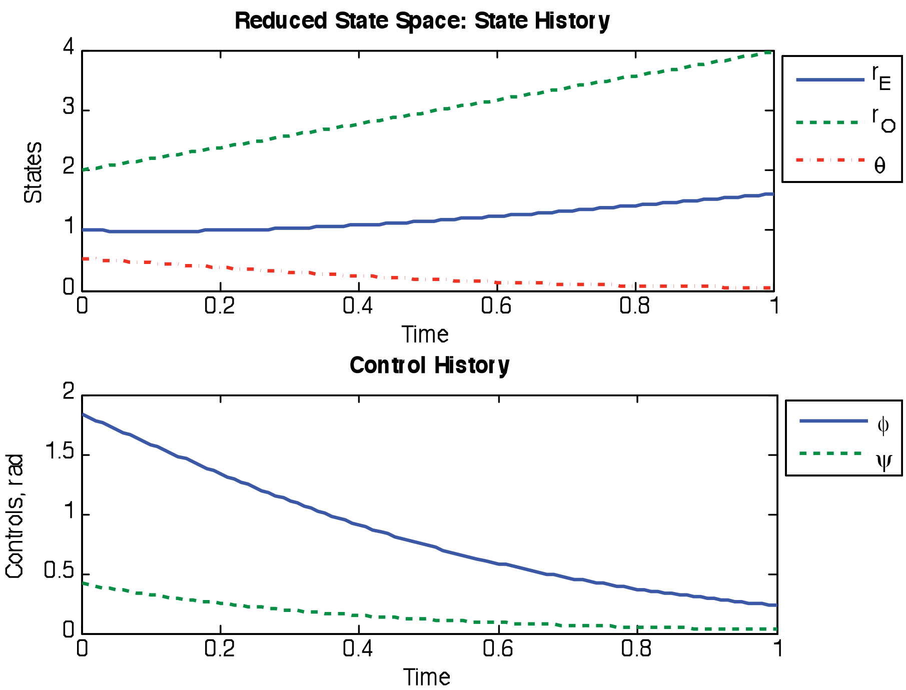

Figure 8. Time History for $\alpha = 2$, $r_{E_0} = 1$, $r_{O_0} = 2$ and $\theta_0 = \frac{\pi}{6}$

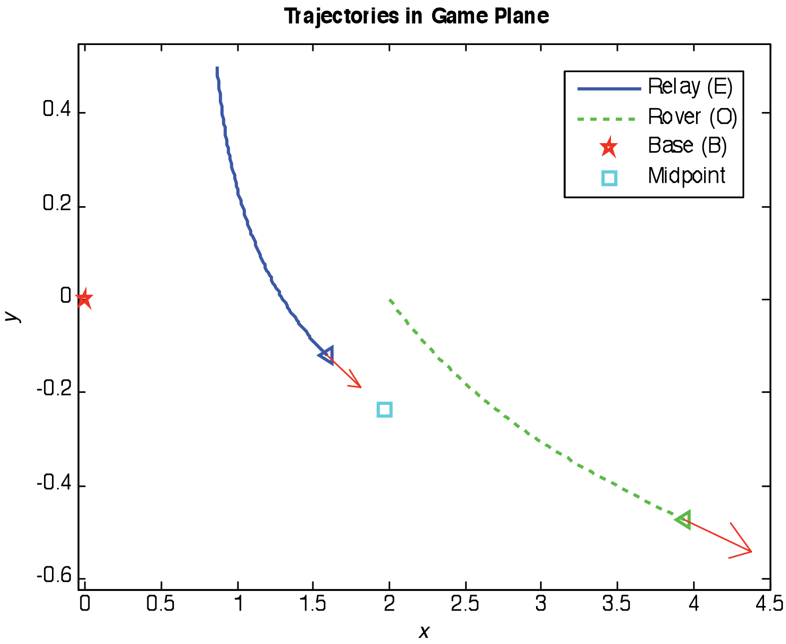

Figure 8. Results for $\alpha = 2$, $r_{E_0} = 1$, $r_{O_0} = 2$ and $\theta_0 = \frac{\pi}{6}$

Once E, B and O are collinear, the reduced Relay velocity eliminates the need for excessive control use. However, it is possible that the Relay might never arrive at the midpoint due to a short planning horizon T, or the maximizing effort of the Rover. If the Rover used a suboptimal control strategy (which is expected in practice), it is then possible for the Relay to arrive at the midpoint and consistently match the motion of the midpoint.

3.2. One-Sided Optimal Control Problem

The following optimal control problem is interesting in its own right and provides insight into the differential game at hand. The complexity of the dynamic optimization problem is significantly reduced by holding one of the MAVs at a fixed position: We will optimize the control of the Relay when the Rover is stationary, that is, $r_O \equiv 1$. Now the parameter $\alpha = 0$ and the state space is reduced to $\mathbf{R}^1 \times \mathbf{S}^1$. The optimal control problem is considered:

$$
\begin{aligned}
&\min_{\varphi} \mathcal{Y} = \int_0^T \left(2r_E^2 + 1 - 2r_E\cos\theta\right)dt \\
&\quad s.t. \\
&\quad \dot{r}_E = \cos\varphi \qquad , \; r_E(0) = r_{E_0} \\
&\quad \dot{\theta} = -\tfrac{1}{r_E}\sin\varphi \;,\; \theta(0) = \theta_0, \;\; 0 \le t \le T
\end{aligned}
\tag{14}
$$

The Hamiltonian is

$$
\mathcal{H} = -2r_E^2 - 1 + 2r_E\cos\theta + \lambda_{r_E}\cos\varphi - \lambda_\theta \tfrac{1}{r_E}\sin\varphi \tag{15}
$$

According to the Pontryagin Maximum Principle[3], the differential equations for the co-states are

$$
\begin{aligned}
\dot{\lambda}_{r_E} &= 4r_E - 2\cos\theta - \frac{\lambda_\theta \sin\varphi}{r_E^2} \quad , \; \lambda_{r_E}(T) = 0 \\
\dot{\lambda}_\theta &= 2r_E\sin\theta \qquad\qquad\qquad\quad , \; \lambda_\theta(T) = 0
\end{aligned}
\tag{16}
$$

and the optimality condition is given by $\max_{\varphi} \mathcal{H}$, namely

$$\frac{\partial \mathcal{H}}{\partial \varphi} = -\lambda_{r_E} \sin\varphi - \frac{\lambda_\theta \cos\varphi}{r_E} = 0 \qquad (17)$$
$$\Rightarrow \tan\varphi = -\frac{\lambda_\theta}{\lambda_{r_E} r_E}$$

The second-order sufficiency condition is:

$$\frac{\partial^2 \mathcal{H}}{\partial \varphi^2} = -\lambda_{r_E} \cos\varphi + \frac{\lambda_\theta \sin\varphi}{r_E} < 0 \qquad (18)$$

From Eqs. (17) and (18) we conclude that, as in the differential game,

$$\lambda_\theta(t) < 0 \;\forall\; 0 \le t < T \qquad (19)$$

The expression for φ given in Eq. (17) is used to rewrite the state and co-state equations only in terms of the states and co-states, obtaining the nonlinear TPBVP

$$\begin{aligned}
\dot{r}_E &= \frac{\lambda_{r_E} r_E}{\sqrt{\lambda_{r_E}^2 r_E^2 + \lambda_\theta^2}} && , \; r_E(0) = r_{E_0} \\
\dot{\theta} &= \frac{\lambda_\theta}{r_E \sqrt{\lambda_{r_E}^2 r_E^2 + \lambda_\theta^2}} && , \; \theta(0) = \theta_0 \\
\dot{\lambda}_{r_E} &= 4 r_E - 2\cos\theta + \frac{\lambda_\theta^2}{r_E^2 \sqrt{\lambda_{r_E}^2 r_E^2 + \lambda_\theta^2}} && , \; \lambda_{r_E}(T) = 0 \\
\dot{\lambda}_\theta &= 2 r_E \sin\theta && , \; \lambda_\theta(T) = 0, \; 0 \le t \le T
\end{aligned} \qquad (20)$$

This one-sided optimization problem is easier to solve than the min-max problem initially posed in (10) and can therefore be analyzed using readily available optimization programs. GPOCS is a Matlab-based optimization program that uses the "Gauss pseudospectral method where orthogonal collocation is performed at the Legendre-Gauss points"[6] to find the minimizing path of the Relay in this situation.

For the case of a stationary rover, the following numerical results show the solution of the optimization problem for T = 0.25, $r_{E_0} = 0.5$ and $\theta_0 = \frac{\pi}{6}$; the co-state initial conditions satisfying the terminal constraints are $\lambda_{r_E}(0) = -0.0347$ and $\lambda_\theta(0) = -0.0647$.

[6] Tomlab Optimization Inc., "GPOCS – Optimal Control Software," Retrieved February 19, 2008 from http://gpocs.com

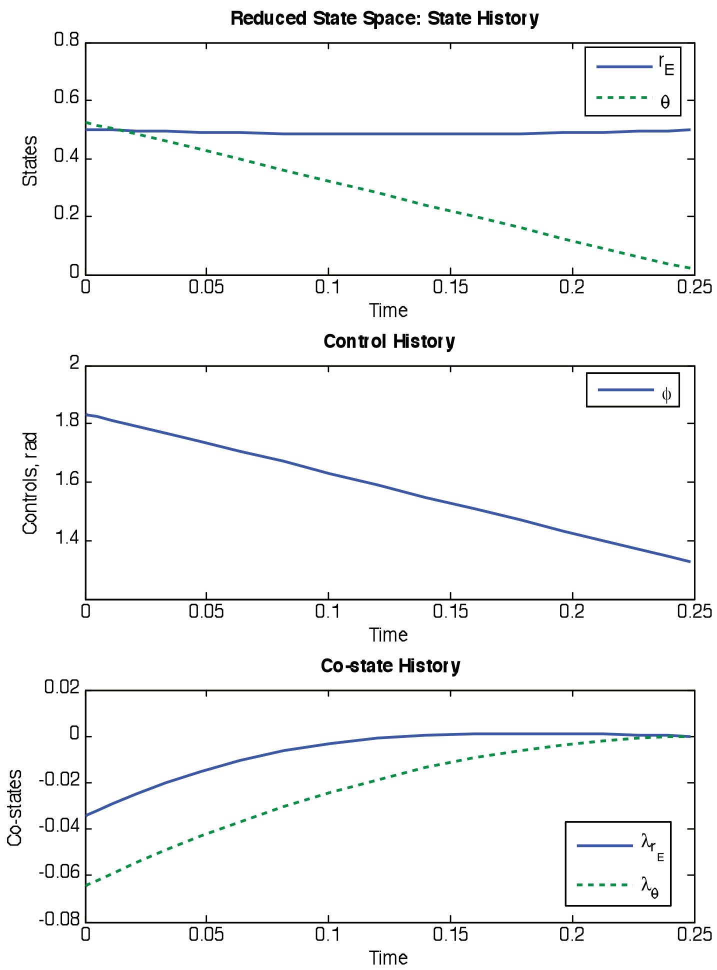

Figure 10. Time History for One-Sided Optimization Problem: $T = 0.25$, $r_{E_0} = 0.5$, and $\theta_0 = \frac{\pi}{6}$

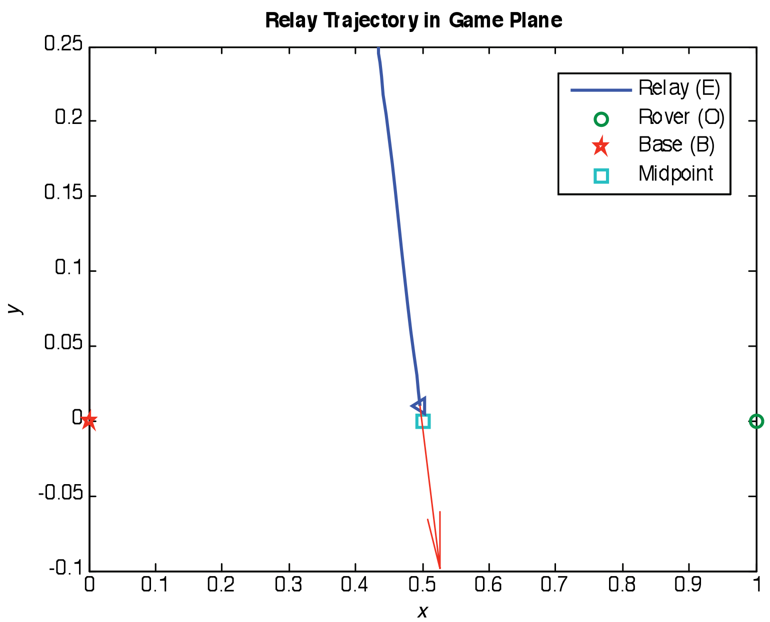

Figure 11. One-Sided Optimization Results for: $T = 0.25$, $r_{E_0} = 0.5$, and $\theta_0 = \frac{\pi}{6}$

It is important to note that the slope of the path traveled by the Relay maintains a constant value of 105° (measured counter-clockwise from the *x*-axis). The numerical results confirm that the Relay travels along the straight-line path toward the midpoint M. This corroborates nicely with the solution found using the geometric approach, namely, the Relay should move directly toward the midpoint.

The following numerical results show the solution of the optimization problem for $T = 0.48$, $r_{E_0} = 0.5$ and $\theta_0 = \frac{\pi}{3}$. The co-state initial conditions satisfying the terminal constraints are $\lambda_{r_E}(0) = -0.257$ and $\lambda_\theta(0) = -0.2165$.

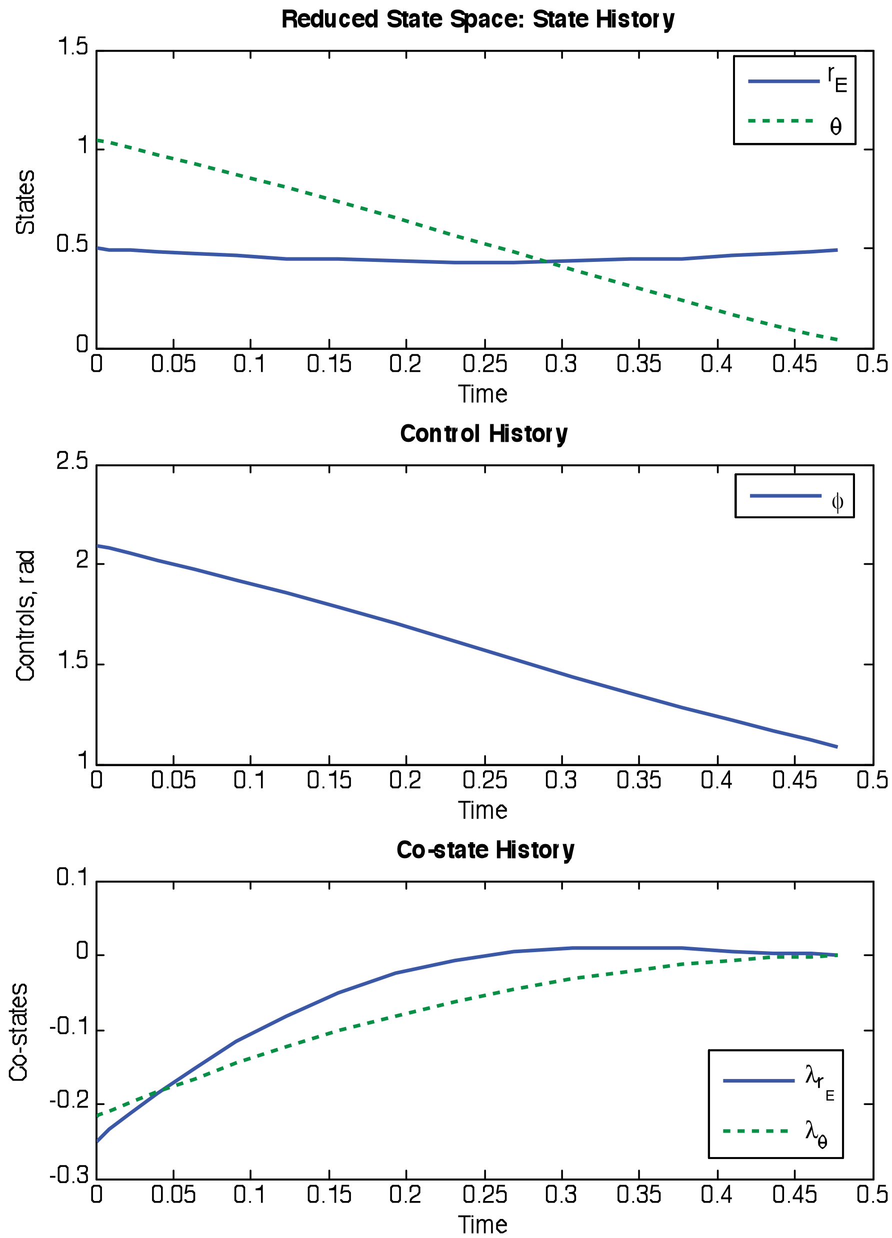

Figure 12. Time History for One-Sided Optimization Problem: $T = 0.48$, $r_{E_0} = 0.5$, and $\theta_0 = \frac{\pi}{3}$

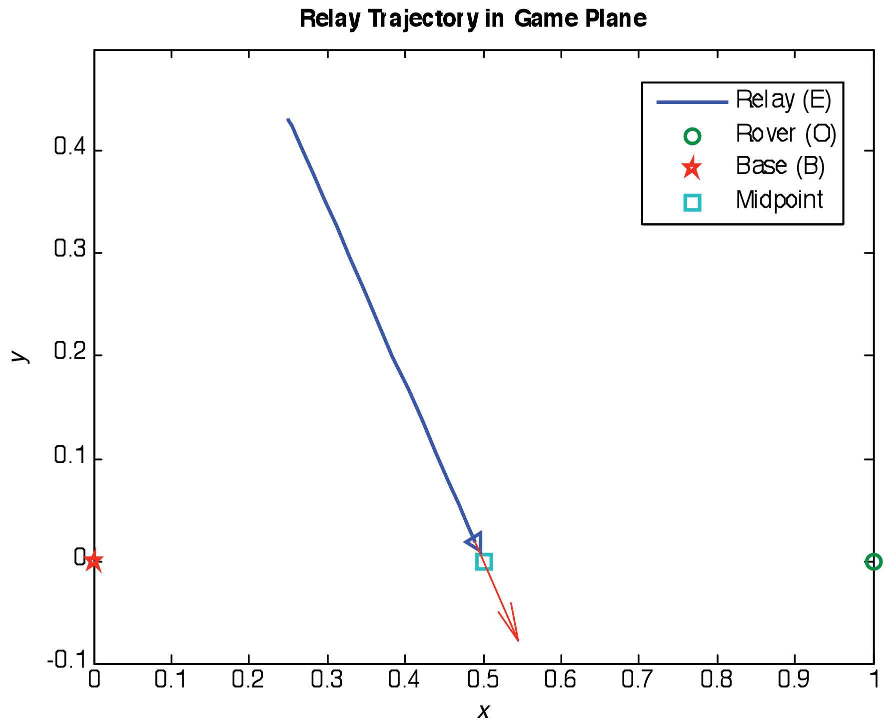

Figure 13. One-Sided Optimization Results for $T = 0.48$, $r_{E_0} = 0.5$, and $\theta_0 = \frac{\pi}{3}$

Similar to the first case, the slope of the path traveled by the Relay maintains a constant value of 120º (measured counter-clockwise from the *x*-axis). The optimal solution is indeed a straight-line path toward the midpoint between the Base and the Rover.

The suboptimal solution and the solution of the one-sided, optimal control problem yielded the respective Relay and Rover strategies: the Relay should head to the midpoint *M* and the Rover should run away from the Relay. These resulted from a myopic analysis of the conflict scenario. Now, during the end-game, it is optimal to be myopic. Therefore, the above strategies are the optimal strategies in the end-game. One reverts to sub-optimality by employing these strategies throughout the game.

4. PLANNING HORIZON/GAME PARAMETER SPACE

The Rover uses the services of the Relay as long as $\overline{OE} < \overline{OB}$, for if $\overline{OE} \geq \overline{OB}$, communication with the Base through the Relay will be counterproductive. In the case where $\overline{OE} = \overline{OB}$, the geometry of the engagement will form an isosceles triangle and the Rover will lie on the orthogonal bisector of $\overline{BE}$ shown by the dashed line in Figure 14.

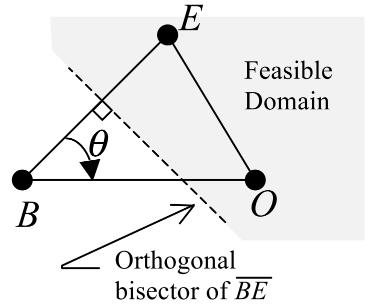

Figure 14. Schematic of Initial Condition Border Line

Therefore, in order to make proper use of the Relay, the state must satisfy the condition

$$0 \le \theta < \cos^{-1}\left(\frac{1}{2}\frac{r_E}{r_O}\right) \tag{21}$$

This defines the bounds of the Feasible Domain depicted in Figure 14.

The optimal solution will make sense, provided that the state satisfies condition (21) $\forall 0 \le t \le 1$. The geometric considerations-based suboptimal strategies in the scenario illustrated in Figure 15 show that eventually, the orthogonal bisector of the segment BE might be crossed by the Rover and hence there must be a maximum planning horizon, depending on the initial values for r_E, r_O and θ. In other words, a time $0 < t_c \le 1$ exists such that condition (21) becomes active. Once the Rover reaches the bisector of the segment BE , condition (21) is violated and the game is over.

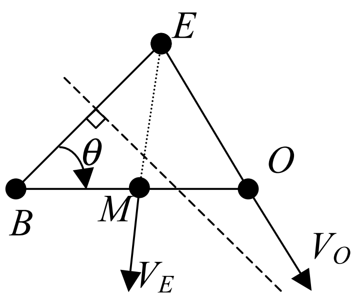

Figure 15. Initial Condition with Limited Planning Horizon

If the initial configureuration/state is as shown in Figure 16, then the maximum possible planning horizon will theoretically approach infinity. That is, condition (21) will not limit the maximum planning horizon; in practice, the planning horizon may still be limited by other factors. For this to be the case, the state must satisfy the following condition for all time.

$$\theta < \cos^{-1}\left(2\frac{r_E}{r_O}\right) \tag{22}$$

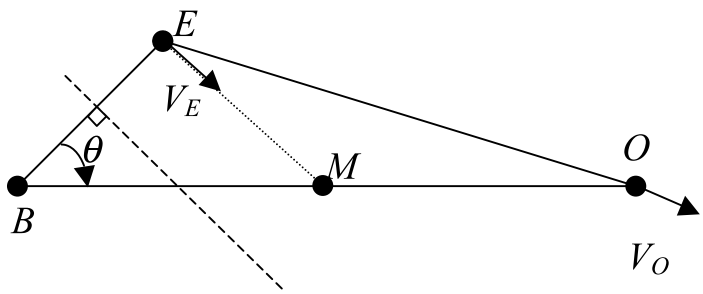

Figure 16. Initial Condition with Unlimited Planning Horizon

The maximum possible planning horizon is unbounded by the relation between $\overline{OE}$ and $\overline{OB}$ when

$$0 < \theta < \cos^{-1}\left(2\frac{r_E}{r_O}\right)$$

and is bounded when

$$\cos^{-1}\left(2\frac{r_E}{r_O}\right) < \theta < \cos^{-1}\left(\frac{1}{2}\frac{r_E}{r_O}\right)$$

5. THE SOLUTION OF THE TPBVP

The suboptimal solutions provide corroborating results, showing that the Relay should fly directly toward the instantaneous midpoint between the Rover and the Base. The optimal control for the Rover to reverse this action would be to fly away from the Relay, as suggested in the suboptimal geometric consideration. Therefore, the initial controls, given an initial state, can be found using the results from the geometric approach. These initial controls are used with Eqs. (6) and (7) to express the initial co-states λ_{r_E} and λ_{r_O} as a function of the initial co-state λ_θ. This reduces the number of unknown initial co-states to one, namely, λ_θ. We also know $\lambda_\theta < 0$.

Choosing a value for λ_θ will provide the two other initial co-state values needed to solve the nonlinear TPBVP given in Eqs. (10) forward in time. Using the values as initial guesses, the correct initial values of the co-states are found using an iterative method, referred to as a "shooting" method. The process for the shooting method is given below.

1. At the iteration step k, the proposed initial co-states ($\lambda_k(0) = \lambda(0)$) are used with the known initial states ($x_k(0) = x(0)$) to obtain a time history of the nonlinear differential system given in Eqs. (10) on the interval $0 \le t \le 1$ using *ode45* in Matlab. This time history will be referred to as $x_k(t)$ and $\lambda_k(t)$. The final value of the co-states in the history is $\lambda_k(T)$.
2. The differential system is then linearized about the trajectory $x_k(t)$, $\lambda_k(t)$, $0 \le t \le 1$ to obtain a time-dependent linear system in the perturbations $\delta x_k(t)$, $\delta\lambda_k(t)$:

$$\frac{d}{dt}\begin{pmatrix} \delta x \\ \delta\lambda \end{pmatrix} = A_k(t)\begin{pmatrix} \delta x \\ \delta\lambda \end{pmatrix},\ \delta x(0) = 0,\ \delta\lambda(0) = \delta\lambda_k,\ 0 \le t \le 1 \tag{23}$$

The A_k matrix is found using the Jacobian function on the differential equations of the system with reference to the states and co-states. Then the values of the states and co-states are substituted into the A_k matrix, resulting in a A_k matrix at each time step.

3. Then, each of the states and co-states are give an initial unit perturbation which is then propagated using the linear differential system to find the resultant change in states and co-states at $t = 1$. This collection of resultant changes is combined to form a resolvent Φ matrix which relates an initial perturbation to a resultant change in state.

$$\begin{pmatrix} \delta x(1) \\ \delta\lambda(1) \end{pmatrix} = \Phi(1)\begin{pmatrix} 0 \\ \delta\lambda_k \end{pmatrix} \tag{24}$$

The Φ matrix can actually be divided into four sub-matrices:

$$\Phi = \begin{bmatrix} \Phi_{1,1} & \Phi_{1,2} \\ \Phi_{2,1} & \Phi_{2,2} \end{bmatrix}$$

so that

$$\delta\lambda(1) = \Phi_{2,2}(1)\delta\lambda_k \tag{25}$$

4. Finally, we calculate the required perturbation of the co-states. Eqs. (10) require that all co-states have a final value equal to zero. Therefore, the goal is for any nonzero final co-state ($\lambda_k(1)$) found in step 1 to be countered by the resultant change in co-state ($\delta\lambda(1)$) found in step 3. Thus

$$\begin{aligned} 0 &= \lambda_k(1) + \delta\lambda(1) \\ &= \lambda_k(1) + \Phi_{2,2}(1)\delta\lambda_k \\ \Rightarrow \delta\lambda_k &= -\Phi_{2,2}^{-1}(1)\lambda_k(1) \end{aligned} \tag{26}$$

Then, by adding the perturbation found in Eq. (26), the proposed co-states for the next iteration are found and eventually one should converge to a final co-state value of zero. Hence, set

$$\begin{aligned} \lambda_{k+1} &:= \lambda_k + \delta\lambda_k \\ \Rightarrow \lambda_{k+1} &= \lambda_k - \Phi_{2,2}^{-1}(1)\lambda_k(1) \end{aligned} \tag{27}$$

The steps in this shooting method are then repeated until the final co-states $\lambda_k(1)$ converge to zero. It is important to note that if the sub-matrix $\Phi_{2,2}(1)$ is not invertible, then the generalized inverse of $\Phi_{2,2}(1)$ should be used:

$$\delta\lambda_k = -\Phi_{2,2}^{\dagger}(1)\lambda_k(1)$$

Specifically, calculate the full rank factorization of $\Phi_{2,2}(1)$.

$$\begin{aligned} &\Phi_{2,2}(1) = HK \\ &\Rightarrow \Phi_{2,2}^{\dagger}(1) = K^T(KK^T)^{-1}(H^TH)^{-1}H^T \end{aligned}$$

The shooting method yields initial co-states which do not equal zero at the end of the planning horizon, $t = 1$. Therefore, the co-states are used as initial guesses for another shooting method program. This program uses *ode45* to solve Eqs. (10) for the same time interval ($0 \le t \le 1$) and iteratively guesses initial conditions for the co-states, using *lsqnonlin*, to minimize the error of the terminal conditions of the co-states, namely, they must equal zero at $t = 1$.

This final shooting method provides the initial co-states which most closely result in satisfaction of the terminal constraints. However, the performance of the program requires a very good initial guess. The first shooting method provides this initial guess. The flow chart shown in Figure 17 provides a visualization to assist in understanding how the results from the geometric approach are used by the aforementioned Matlab programs to attain full system results. The flow represented here is implemented by a single Matlab program: “geometry_applied_rdg.m”.

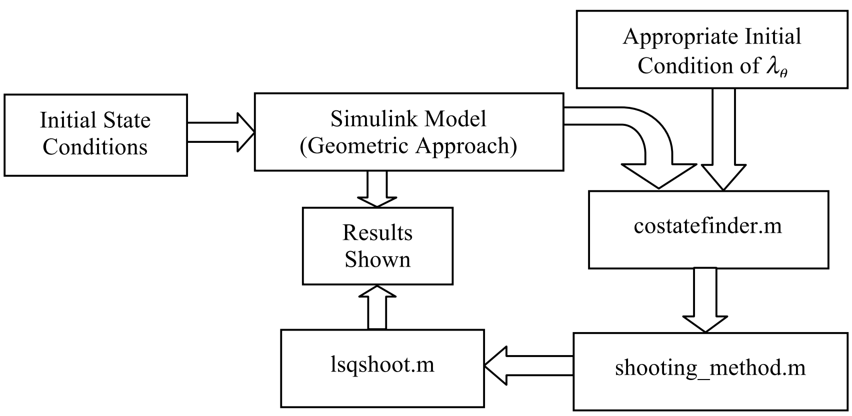

Figure 17. Flow Chart of Matlab Programs Which Produce Full System Results

6. NUMERICAL RESULTS

The nonlinear TPBVP given by Eqs. (10) is solved using the two shooting methods described in the previous section. These shooting methods find the initial co-states by using the data obtained from the geometric approach with Eqs. (6) and (7), and an appropriate value for λ_θ. To provide an easier comparison, the game plane results of the geometric approach are repeated with the results found using the shooting methods in the figureures below.

The following numerical results illustrate the evolution of the differential game in the case where the parameter $\alpha = 1$ and the initial conditions are $r_{E_0} = 2$, $r_{O_0} = 4$ and $\theta_0 = \frac{\pi}{6}$. The co-state initial conditions which most closely satisfy the terminal constraints are $\lambda_{r_E}(0) = -0.2941$, $\lambda_{r_O}(0) = -5.0271$ and $\lambda_\theta(0) = -5.3574$. The resulting terminal co-states are $\lambda_{r_E}(T) = -0.0029$, $\lambda_{r_O}(T) = -0.0022$ and $\lambda_\theta(T) = -0.0000$

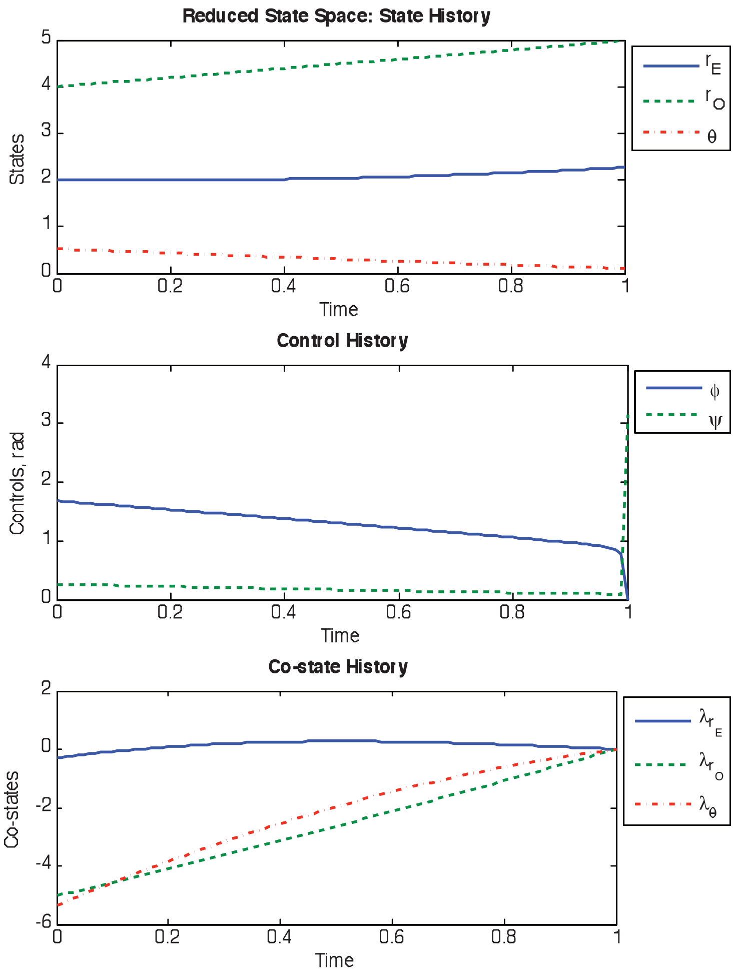

Figure 18. Time History for $\alpha = 1$, $r_{E_0} = 2$, $r_{O_0} = 4$ and $\theta_0 = \frac{\pi}{6}$

The optimal trajectories differ from the geometric approach-provided trajectories, but the geometric approach is suboptimal. This may be the closest result to an optimal solution to the differential game for the given initial condition, since the second-order sufficiency conditions (given by Eqs. (8) and (9)) are satisfied and the terminal co-states are very near zero. It appears that the Relay is still heading toward M, but the Rover's strategy has changed somewhat.

The following numerical results illustrate the evolution of the differential game in the case where the parameter $\alpha = 1$ and the initial conditions are $r_{E_0} = 1$, $r_{O_0} = 2$ and $\theta_0 = \frac{\pi}{3}$. The co-state initial conditions which most closely satisfy the terminal constraints are $\lambda_{r_E}(0) = -1.1146$, $\lambda_{r_O}(0) = -3.3284$, and $\lambda_\theta(0) = -2.5645$. The resulting terminal co-states are $\lambda_{r_E}(T) = -0.0001$, $\lambda_{r_O}(T) = -0.0000$.

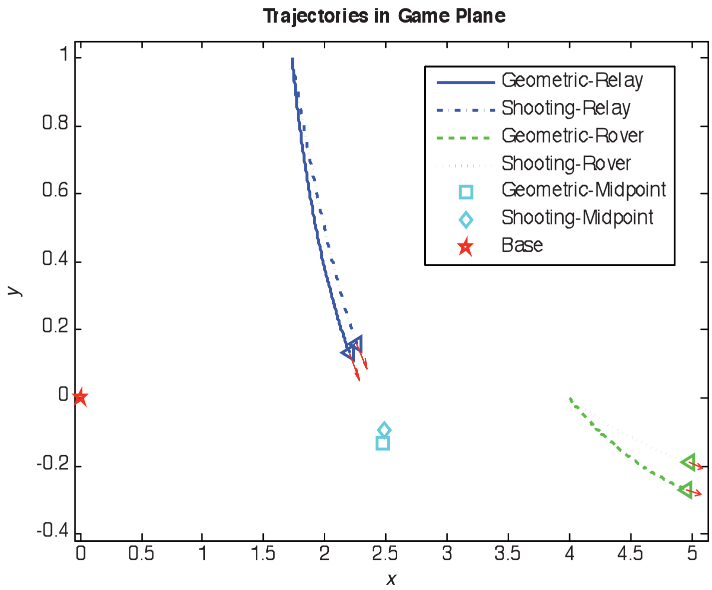

Figure 19. Comparative Results for $\alpha = 1$, $r_{E_0} = 2$, $r_{O_0} = 4$ and $\theta_0 = \frac{\pi}{6}$

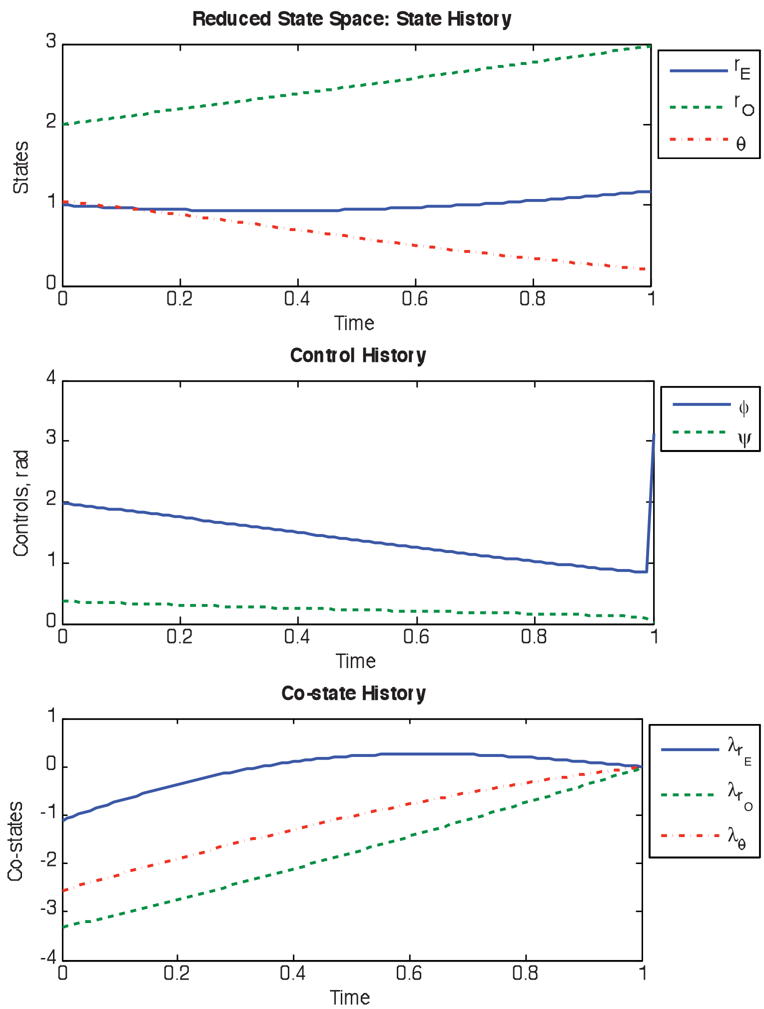

Figure 20. Time History for $\alpha = 1$, $r_{E_0} = 1$, $r_{O_0} = 2$ and $\theta_0 = \frac{\pi}{3}$

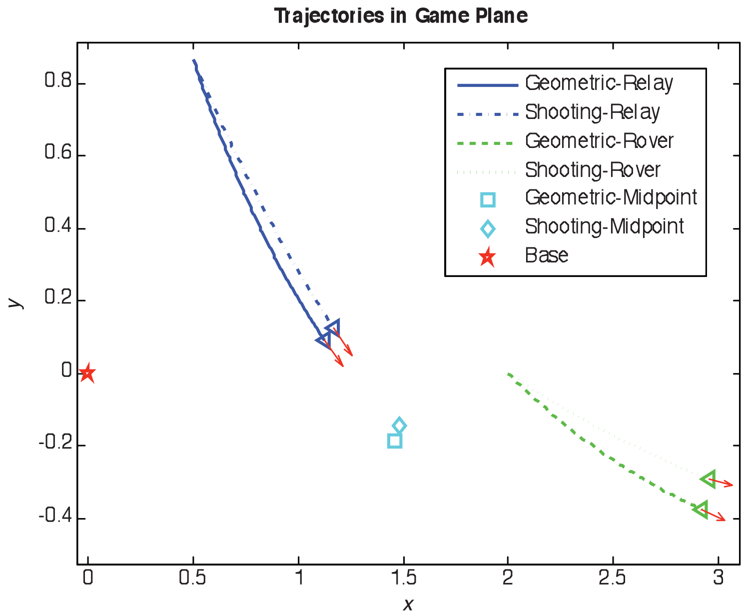

Figure 21. Comparative Results for $\alpha = 1$, $r_{E_0} = 1$, $r_{O_0} = 2$ and $\theta_0 = \frac{\pi}{3}$

These results also differ from the geometric approach, but they are consistent with the near-optimal solution found in the first scenario. This provides corroboration for identifying the optimal solution because the solutions to each scenario exhibit similar behavior, satisfy the second-order sufficiency conditions (given by Eqs. (8) and (9)), and have near-zero terminal co-state values.

The following numerical results illustrate the evolution of the differential game in the case where the parameter $\alpha = 2$ and the initial conditions are $r_{E_0} = 1$, $r_{O_0} = 2$ and $\theta_0 = \frac{\pi}{6}$. The co-state initial conditions which most closely satisfy the terminal constraints are The resulting terminal co-states are $\lambda_{r_E}(0) = -0.2888$, $\lambda_{r_O}(0) = -3.4600$, and $\lambda_\theta(0) = -1.4658$. The resulting terminal co-states are $\lambda_{r_E}(T) = 0.0425$, $\lambda_{r_O}(T) = -0.0046$ and $\lambda_\theta(T) = -0.0000$.

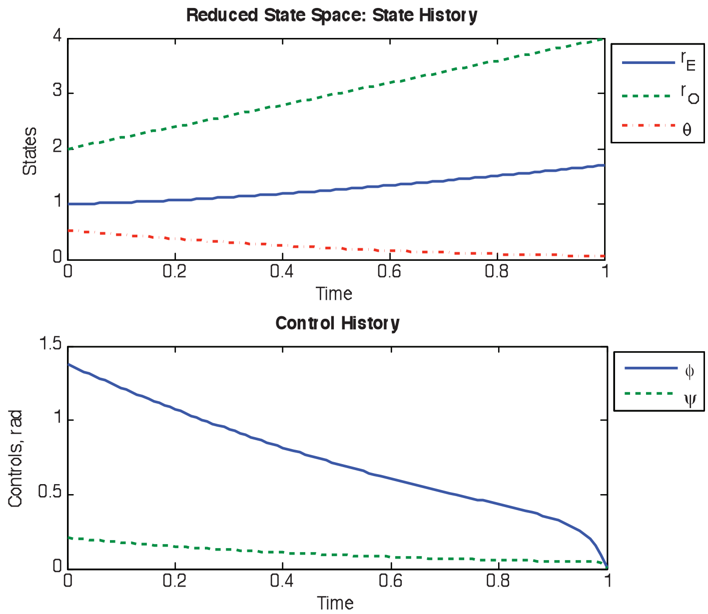

Figure 22. (continued)

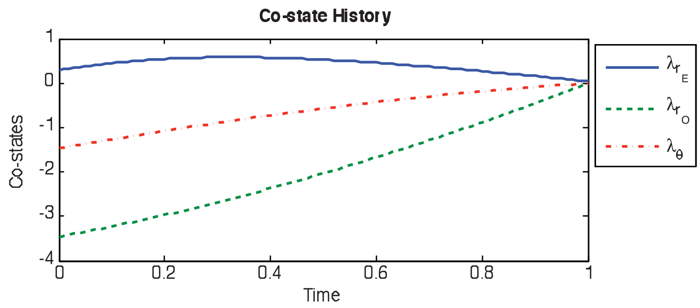

Figure 22. Time History for $\alpha = 2$, $r_{E_0} = 1$, $r_{O_0} = 2$ and $\theta_0 = \frac{\pi}{6}$

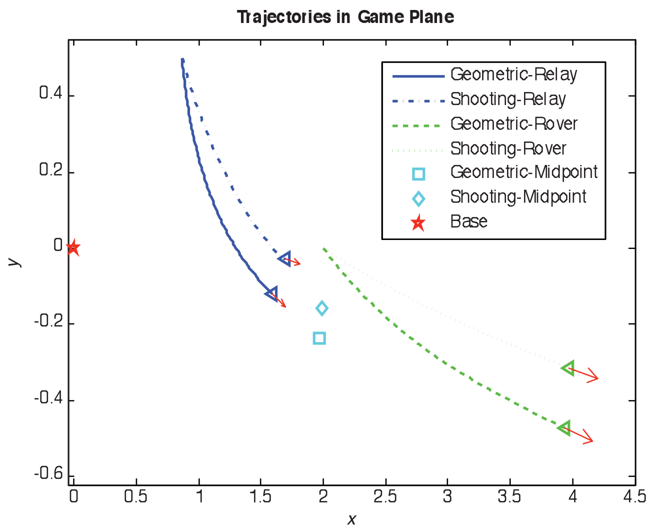

Figure 23. Comparative Results for $\alpha = 2$, $r_{E_0} = 1$, $r_{O_0} = 2$ and $\theta_0 = \frac{\pi}{6}$

These results also corroborate with the first two scenarios, except that the Relay appears to depart from its strategy near the end. This may be a result of the terminal co-states having greater deviation from zero than in the first two numerical results. However, since this scenario represents a special case ($\alpha = 2$) where the Relay moves at the same speed as M, the results are possibly due to the physics present in the system. The second-order sufficiency conditions (given by Eqs. (8) and (9)) are still satisfied. This provides incentive for further research of this special case of the differential game and the nonlinear TPBVP given by Eq. (10).

CONCLUSIONS

This paper developed optimal guidance laws for a Relay MAV in support of extended range ISR. The guidance laws are based upon the solution of a min-max optimization problem, namely, the solution of the differential game, which represents a worst case scenario. The solution of the differential game hinges on the solution of a nonlinear TPBVP. Suboptimal Relay (and Rover) guidance strategies are first provided. The first of these suboptimal guidance strategies is derived using a geometry-based (sub)optimality principle: the Relay heads toward the instantaneous midpoint of the straight line between the Rover and the Base. The Rover, heads directly away from the Relay. The respective strategies of heading toward the midpoint, M, and running away from the Relay are the optimal strategies in the end-game. The second suboptimal guidance strategy is derived from the solution to a one-sided Relay optimal control problem, where the Rover is considered stationary. The results obtained using the Matlab optimization program GPOCS showed that the optimal guidance law of the Relay is to fly directly toward the instantaneous midpoint of the straight line between the Rover and the Base. The heuristic methods provided corroborating results which were then used as first guesses for a combination of two shooting methods applied in tandem to solve the TPBVP in order to obtain the solution of the differential game. The shooting method results yielded the numerical solution of the Relay-Rover differential game.

Future work will address the mitigation of deleterious effects of communication delays in the Relay's state feedback control law. These effects are brought about by a degree of tardiness in reporting the Rover's current position. This is an important step towards a planned flight test in the near future, and eventual implementation.

APPENDIX A - GEOMETRY

An Elementary Euclidean Geometry Result

It is well known that the locus of all points such that the sum of the distances from two fixed points is constant, is an ellipse. Thus, the following is of some interest.

Theorem 1 The Locus of all points such that the sum of the *squares* of the distances from two fixed points is constant, is a circle centered at the midpoint of the segment formed by the two fixed points. The radius of this circle is

$$R = \sqrt{d^2 - f^2}$$

where the sum of the squares of the distances is $2d^2$ and the distance between the fixed points is $2f$; obviously, $d \geq f$.

Proof:

Let the fixed points F_1 and F_2 be on the x-axis ($F_1 = (f, 0)$, $F_2 = (-f, 0)$) as shown in the figure below.

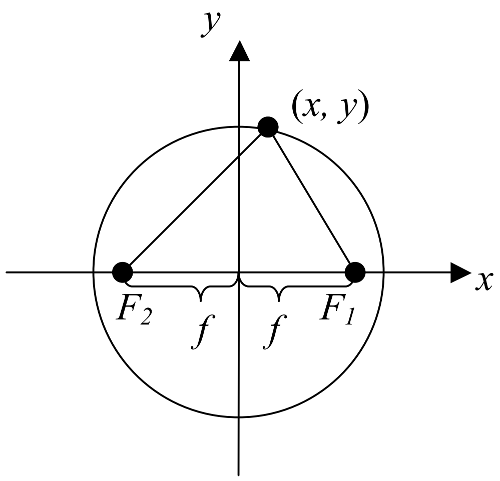

Figure 24. Schematic of Fixed Points Showing Isocost Circle

The sum of the squares of the distances is calculated as

$$\begin{aligned} 2d^2 &= (f + x)^2 + y^2 + (f - x)^2 + y^2 \\ &= 2f^2 + 2x^2 + 2y^2 \\ \Rightarrow \quad & x^2 + y^2 = d^2 - f^2 \end{aligned}$$

This is the equation of a circle centered at the origin, whose radius is

$$R = \sqrt{d^2 - f^2}$$

This result appeared in Ref. 4.

Remark: The loci of constant costs, $2d^2$, are concentric circles where the minimum cost is found at the midpoint of the line formed by F_1 and F_2, where $d = f$.

Extension: The Locus of all points such that the weighted sum of the squares of the distances from two fixed points is constant, is a circle centered on the segment formed by the two fixed points and is at a distance of $(1 - 2w)f$ from this segment's midpoint. The radius of this circle is

$$R = \sqrt{d^2 - 4w(1-w)f^2}$$

where d^2 is the specified weighted sum of the squares of the distances, the distance between the fixed points is $2f$; and the weight is w; if $w < 0$ or $w > 1$ this is true $\forall d > 0$, and if $0 \le w \le 1$, $d > 2f\sqrt{w(1-w)}$, Note: When the weight $w = ½$, need $d > f$.

Proof:

The weighted sum of the squares of the distances is calculated as

$$\begin{aligned} d^2 &= w\left[(f+x)^2 + y^2\right] + (1-w)\left[(f-x)^2 + y^2\right] \\ &= wf^2 + wx^2 + 2wfx + wy^2 + (1-w)f^2 + (1-w)x^2 - 2(1-w)fx + (1-w)y^2 \\ &= f^2 + x^2 + y^2 - 2fx(1-2w) \\ &= \left[x - (1-2w)f\right]^2 + f^2 + y^2 - (1-2w)^2 f^2 \\ &\Rightarrow \left[x - (1-2w)f\right]^2 + y^2 = d^2 - 4w(1-w)f^2 \end{aligned}$$

REFERENCES

[1] Dixon, C. R. and Frew, E. W., "Cooperative Electronic Chaining Using Small Unmanned Aircraft," In *AIAA Infotech@Aerospace*, AIAA, Rohnert Park CA, May 2007.

[2] Goldenberg, D., Lin, J., Morse, A. S., Rosen, B. E., and Yang, Y. R., "Towards Mobility as a Network Control Primitive," In *ACM Mobihoc '04*, Tokyo Japan, 24-26 May 2004.

[3] L. S. Pontryagin, V. G. Boltyanskii, R. V. Gamkrelidze, and E. F. Mishchenko, *The Mathematical Theory of Optimal Processes*, John Wiley, New York, 1962.

[4] V. Gutenmacher and N. B. Vasilyev, *Lines and Curves*, Birkhäuser Boston, Boston MA, 2004, pp. 23-24.

[5] T. Shima and S. Rasmussen, Editors. *UAV Cooperative Decision and Control*, SIAM, Philadelphia, 2009.

[6] M. Hirsch, C. Commander, P. Pardolos and R. Murphey, *Optimization and Cooperative Control Strategies*, Lecture Notes in Control and Information Sciences, Vol. 381, Springer, (2009).

[7] P. Pardolos, D. Grundel and R. Murphey, editors. *Cooperative Networks – Control and Optimization*, Oleg Prokopyev Edward Elgar Publishing, (2008).

[8] D. Grundel, R. Murphey, P. Pardolos and O. Prokpyev, editors. *Cooperative Systems – Control and Optimization*, Springer, (2007).

[9] M. Hirsch, P. Pardolos, R. Murphey and D. Grundel, editors. *Advances in Cooperative Control and Optimization*, Springer, (2006).